Reflection and transmission coefficients in TI media: exact and linearized phase velocities, eikonals and polarization vectors

Patrick F. Daley, Edward S. Krebes, and Lawrence R. Lines

ABSTRACT

Reflection and transmission coefficients which partition energy due to plane wave incidence at the interface between two transversely isotropic (TI) media are considered. The basic forms of these coefficients employed use expressions for certain quantities that may be classified as either exact or linearized. Phase velocities and the related slowness vectors, as well as the polarization vectors for the incident and the four possible reflected or transmitted wave types, are investigated for both levels of accuracy mentioned above. Computed results for these precision types should be compared graphically for what has been termed weak anisotropy (WA). However, liberties will be taken and at least one of the media will be chosen to be strongly anisotropic, to determine the possible limits of the degree of anisotropy which may be considered without a major compromise of results. The results suggest that the degree of anisotropy, for which the linearized quantities are assumed to provide reasonably accurate results, may be larger than that typically associated with "weakly anisotropic" media. A full sensitivity study is not done here as the prime motivation for this work was to develop the linearized formulation of reflection and transmission coefficients, given that the exact solutions are known. This is one of the motivations for undertaking this study, as a linearized algorithm to determine reflection and transmission coefficients for more complex anisotropic media is a future objective.

INTRODUCTION

In the past several decades, the study of elastic wave propagation in complex anisotropic media types has produced necessary supplements to seismic prospecting tools related to the detection of hydrocarbons in geological structures. Methods have been pursued to minimize the mathematical complexity of the formulae involved while still preserving a reasonable level of accuracy. One of these, perturbation theory, has been shown to be a useful tool for the study of wave properties in complex weakly anisotropic media. Formulae for kinematic quantities such as phase velocity and dynamic properties like polarization vectors take on forms which are only moderately more complicated than those for isotropic media, using just a first order approximation (Jech and Pšenčík, 1989, Sayers, 1994, Mensch and Rasolofosaon, 1997, Pšenčík and Gajewski, 1998, Pšenčík and Farra, 2005, and Farra and Pšenčík 2008).

In the paper by Farra and Pšenčík (2003) the extension of perturbation methods to obtain higher order approximations for the phase velocity and polarization vectors for waves of all three types (quasi-compressional, qP, and the two coupled quasi-shear wave modes, qS_1 and qS_2) were discussed. The papers cited in the previous two paragraphs are a sampling rather than an exhaustive list of works on this topic. Readers are directed to the above where other references may be found.

The basic premise of perturbation theory involves starting with some reference velocity, often an isotropic background velocity, and perturb it as $a_{ijkl} = \left[a_{ijkl} \right]_{iso} + \Delta a_{ijkl}$, where the $\left[a_{ijkl} \right]_{iso}$ are just the isotropic equivalents of the anisotropic parameters a_{ijkl}, with anisotropy introduced through the addition of the Δa_{ijkl} terms. The density normalized anisotropic parameters, a_{ijkl} and Δa_{ijkl}, have the dimensions of velocity squared, so that $a_{ijkl} = c_{ijkl} / \rho$, with c_{ijkl} being the stiffness coefficients of the medium, and ρ being the density (Červený , 2001). Once established, this approximation may be introduced into the equations for elastic wave propagation in anisotropic media and manipulated in a standard manner (Jech and Pšenčík, 2008, as an example) starting with substituting c_{ijkl} into the equations of particle motion as

$$\frac{\partial}{\partial x_i}\left(\left[c_{ijkl} \right]_{iso} \frac{\partial u_k}{\partial x_\ell} \right) + \frac{\partial}{\partial x_i}\left(\Delta c_{ijk\ell} \frac{\partial u_k}{\partial x_\ell} \right) - \rho \frac{\partial^2 u_j}{\partial t^2} = 0 \qquad (1)$$

Assuming the zero order asymptotic ray series solution for (1) to be

$$\mathbf{u}(x_i, t) = \mathbf{U}(x_i) \exp\left[-i\omega \left(t - \tau(x_i) \right) \right], \qquad (2)$$

in terms of the slowness vector components p_j $\left(p_j = \partial \tau / \partial x_j,\ j = 1,2,3 \right)$, the following identity results

$$a_{ijk\ell} p_i p_\ell U_k - U_j = 0 \qquad (3)$$

with $a_{ijkl} = c_{ijkl} / \rho = \left[a_{ijkl} \right]_{iso} + \Delta a_{ijkl}$. Time is indicated by "$t$", circular frequency as "ω", the coordinate dependent phase function which describes a wave fronts propagation through a medium as "$\tau(x_j)$" and $\mathbf{U} = (U_1, U_2, U_3)$ the displacement vector. Alternatively, equation (3) may be written as

$$\left(\Gamma_{jk}(x_v, p_v) - \delta_{jk} \right) U_k = 0 \quad \text{with} \quad \Gamma_{jk}(x_v, p_v) = a_{ijk\ell} p_i p_\ell , \qquad (4)$$

so that (4) in terms of the polarization vector has the form

$$\left[\Gamma_{jk}(x_v, p_v) - G\delta_{jk} \right] g_k = 0 . \qquad (5)$$

The Christoffel matrix $\Gamma_{jk}(x_v, p_v)$ is symmetric and positive definite (Červený , 2001). Thus for any direction of the wave vector n_i, which is normal to the qP wave surface, $\Gamma_{jk}(x_v, p_v)$ has three positive and real eigenvalues $G_\zeta = 1$ $(\zeta = 1,2,3)$ and three corresponding unit eigenvectors $\mathbf{g}_\zeta(n_i)$ which satisfy the system of equations (5).

Two eigenvalues G_1 and G_2, with related eigenvectors $\mathbf{g}_1$ and $\mathbf{g}_2$, correspond to the two qS waves, and the remaining eigenvalue G_3, with the eigenvector $\mathbf{g}_3$, is associated with the qP wave. The eigenvalues are related to the squares of corresponding phase velocities $v_\zeta(x_i,n_i)$ as $G_\zeta - v_\zeta^2(x_i,n_i)=0 \quad (\zeta=1,2,3)$ where the relationship $p_i = n_i/v_\zeta(x_j,n_j)$ has been introduced. The above requires that a modified definition of Γ_{jk} be used, so that $\Gamma_{jk}=\Gamma_{jk}(x_\upsilon,n_\upsilon)$. The parameter list for Γ_{jk} will be retained throughout to avoid any confusion, unless the notation is especially clear.

The eigenvectors $\mathbf{g}_m$ specify polarization vectors of the corresponding waves. The eigenvalues G_1 and G_2 have in general, for most geological media, magnitudes less than G_3 (Schoenberg and Helbig, 1997). G_2 will not be used here as in the TI case it corresponds to the G_{qS_V} wave which in a TI medium is decoupled from the coupled wave type pair G_{qP} and G_{qS_V}. Its polarization vector is aligned normal to the plane of ray propagation.

In perturbation formulas of any order, an important role is played by a matrix, $B_{mn}(x_\upsilon,n_\upsilon)\,(m,n=1,2,3)$, whose elements define various attributes of elastic wave propagation, and which is used to obtain other related expressions. Explicit expressions for the elements for one of various possible specifications of the matrix $B_{mn}(x_\upsilon,n_\upsilon)$ used in the literature that are required here, are given in Voigt notation of the anisotropic parameters $A_{ij}\,(i,j=1,2,\ldots,6)$. The anisotropic parameters, A_{ij}, are related to more general anisotropic parameters $a_{ijk\ell}$ (see for example Gassmann, 1964, page 98)) and have the dimensions of velocity squared.

Initially three mutually orthogonal unit vectors are introduced

$$\mathbf{e}_i = (e_{i1},e_{i2},e_{i3}) \quad (i=1,2,3). \tag{6}$$

The vectors $\mathbf{n}$, $\mathbf{e}_1$ and $\mathbf{e}_2$, the relationships of the general components of the $\mathbf{e}_i$ to the components of the vector $\mathbf{n}$ and their degenerate TI forms, are specified in terms of the polar angle, θ, and the azimuthal angle, ϕ, as

$$\begin{aligned}
&\mathbf{n}=\mathbf{e}_3=(e_{31},e_{32},e_{33})=(\sin\theta\cos\phi,\sin\theta\sin\phi,\cos\theta)\\
&\mathbf{n}=(n_1,n_2,n_3)\\
&\mathbf{n}_{TI}=(\mathbf{e}_3)_{TI}=(e_{31},e_{32},e_{33})=(\sin\theta,0,\cos\theta)
\end{aligned} \tag{7}$$

$$\begin{aligned}
\mathbf{e}_1 &= \left(e_{11}, e_{12}, e_{13}\right) = \left(\cos\theta\cos\phi, \cos\theta\sin\phi, -\sin\theta\right) \\
\mathbf{e}_1 &= \left(n_1 n_3, n_2 n_3, n_3^2 - 1\right) D^{-1} \\
\left(\mathbf{e}_1\right)_{TI} &= \left(e_{11}, e_{12}, e_{13}\right) = \left(\cos\theta, 0, -\sin\theta\right) = \left(n_3, 0, -n_1\right)_{TI}
\end{aligned} \tag{8}$$

$$\begin{aligned}
\mathbf{e}_2 &= \left(e_{21}, e_{22}, e_{23}\right) = \left(-\sin\phi, \cos\phi, 0\right) \\
\mathbf{e}_2 &= \left(-n_2, n_1, 0\right) D^{-1} \\
\left(\mathbf{e}_2\right)_{TI} &= \left(e_{21}, e_{22}, e_{23}\right) = \left(0, 1, 0\right)
\end{aligned} \tag{9}$$

where $\mathbf{e}_3 = \mathbf{n}$, $D = \left(n_1^2 + n_2^2\right)^{1/2}$, $n_1^2 + n_2^2 + n_3^2 = 1$ and the vectors $\mathbf{e}_1$ and $\mathbf{e}_2$ specify a plane normal to $\mathbf{n}$. (Figure 1). As these two vectors may be chosen arbitrarily, it will be required that $\mathbf{n}$ and $\mathbf{e}_1$ define the plane in which the rays, which transport energy from one point in a medium to another, are located in a transversely isotropic medium. Due to the rotational invariance of a TI about the vertical, x_3 axis, this plane may be taken at any azimuth. Consequently, the azimuthal angle, $\phi = 0$ has been chosen for use here.

The definition of the matrix B_{mn} used here is defined as

$$B_{mn}\left(x_\upsilon, n_\upsilon\right) = \Gamma_{jk}\left(x_\upsilon, n_\upsilon\right) e_{mj} e_{nk} \quad \text{with} \quad \Gamma_{jk}\left(x_\upsilon, n_\upsilon\right) = a_{ijk\ell} n_i n_\ell \,. \tag{10}$$

It is clear that the vectors $\mathbf{e}_i$ rather than slowness vectors are used here to define a matrix $B_{mn}\left(x_\upsilon, n_\upsilon\right)$ due to the difference in definition of $\Gamma_{jk} = \Gamma_{jk}\left(x_\upsilon, n_\upsilon\right)$ above and that given in equation (4). Development of analytic expressions for individual terms of the matrix $B_{mn}\left(x_\upsilon, n_\upsilon\right)$ will be introduced as required in later sections.

It should finally be noted that Backus (1965) presented the linearized form of the square of the quasi – compressional (qP) phase velocity in a general anisotropic medium, which may be seen to be equal to $B_{33}\left(x_\upsilon, n_\upsilon\right)$, as

$$v_{qP}^2\left(x_\upsilon, n_\upsilon\right) = a_{ijk\ell} n_i n_j n_k n_\ell = \Gamma_{jk}\left(x_\upsilon, n_\upsilon\right) n_j n_k \,, \tag{11}$$

where, $\Gamma_{jk}\left(x_\upsilon, n_\upsilon\right)$ is the form of the Christoffel matrix specified by (10).

THEORY

The paper by Graebner (1992) presents a matrix formulation of the problem of plane wave incidence at the interface between two transversely isotropic media. When solved, the 16 possible reflection and transmission coefficients result. That paper was initially used as the effect of the polarization vectors on the matrix elements may be seen quite clearly. The closed form solution of the matrix equation presented in that paper was

derived in a subsequent unpublished work by the authors; the resulting analytic expressions for the coefficients were left in forms that were not fully developed so that the effects of the polarization vector components on individual coefficients could be analyzed at a later time.

The intent of this work is to compare the reflection and transmission coefficients for two of the most widely used coefficients, R_{P1P1} and R_{P1S1}, when linearized quantities are introduced to replace the exact polarization vector components. For consistency, linearized phase velocities and eikonals are also incorporated. Expressions for the exact polarization vectors were taken from Daley and Hron (1977), and were with minor changes introduced into the computer code that resulted from the solution of the equations given in Graebner (1992). The linearized forms of the polarization vectors will be discussed in due course. The incident (upper) medium is highly anisotropic, and the lower medium is chosen to be isotropic so that any anisotropic effects are due to the anisotropy in the upper medium.

As a reference point, the exact expressions for the polarization vectors, $\mathbf{g}_{qP/qS_V}$, related to the coupled $qP-qS_V$ wave propagation in an isotropic medium, may be written as

$$\mathbf{g}_{\varsigma} = \left(\sin\theta_{\varsigma}, \pm\cos\theta_{\varsigma}\right) \tag{12}$$

where ς is either "$0(n)$" *or* "n" with n = 1,2,3,4 and the perturbed expression due to the introduction of anisotropy is of the form

$$\mathbf{g}_{\varsigma} = \left(g^1_{\varsigma}, g^3_{\varsigma}\right) = \left(\sin\theta_{\varsigma}, \pm\cos\theta_{\varsigma}\right) + \Delta\mathbf{g}_{\varsigma}\,. \tag{13}$$

The subscript ς indicates an incident wave type if it is the form $O(n)$, where $n=1$ refers to a qP wave in the upper (1) medium, $n=2$ to a qS_V wave in the upper (1) medium, $n=3$ to a qP wave in the lower (2) medium, and $n=4$ to a qS_V wave in the lower (2) medium (Figure 2). The notation $O(j)$ indicates an incident wave type at the interface.

In the somewhat more complex transversely isotropic (TI) medium the polarization vectors have the exact form (Daley and Hron, 1977)

$$\mathbf{g}_{qP} = \left(g^1_{(qP)}, g^3_{(qP)}\right), \quad \mathbf{g}_{qS_V} = \left(g^1_{(qS_V)}, g^3_{(qS_V)}\right) \tag{14}$$

where

$$g^1_{(qP)} = \left[\frac{Q + A^{(-)}_{\alpha}}{2Q}\right]^{1/2}, \quad g^1_{(qP)} = \left[\frac{Q - A^{(-)}_{\alpha}}{2Q}\right]^{1/2}. \tag{15}$$

and

$$Q = \left[A_\alpha^2 + 4 A_D p_1^2 p_3^2 \right]^{1/2} = A_\alpha \left[1 + 4\eta_D \right]^{1/2} \quad , \quad \eta_D = \frac{A_D p_1^2 p_3^2}{A_\alpha^2} \quad . \tag{16}$$

Quantities requiring definition are

$$A_\alpha^{(-)} = \left(A_{11} - A_{55} \right) p_1^2 - \left(A_{33} - A_{55} \right) p_3^2 \tag{17}$$

and

$$A_\alpha = \left(A_{11} - A_{55} \right) p_1^2 + \left(A_{33} - A_{55} \right) p_3^2 \quad . \tag{18}$$

with the deviation from the elliptical case given by

$$A_D = \left(A_{11} + A_{13} \right)^2 - \left(A_{11} - A_{55} \right)\left(A_{33} - A_{55} \right) \quad . \tag{19}$$

Its dimensionless form is

$$\tilde{A}_D = \frac{\left(A_{11} + A_{13} \right)^2 - \left(A_{11} - A_{55} \right)\left(A_{33} - A_{55} \right)}{2 A_{33} \left(A_{33} - A_{55} \right)} = \sigma \quad , \tag{20}$$

and in terms of Thomsen's (1986) (ε, δ) notation, $\sigma = \delta - \varepsilon$, with the dimensionless ellipticity defined as $\varepsilon = \left(A_{11} - A_{33} \right) / 2A_{33}$. The slowness vector related to a certain mode of wave propagation, γ, is $\mathbf{p}_\gamma = \left(p_\gamma^1, 0, p_\gamma^3 \right) = \left(p_\gamma^1, p_\gamma^3 \right)$, $(\gamma = qP \text{ or } qS_V)$. It should be noted that the components of the vectors $\mathbf{g}_\zeta$ have been defined only accurate to within a $\pm$ sign. This fact may be seen more clearly in Figure (2) , which has been redrawn from Daley and Hron (1977).

Figure (2) displays the orientations of all components of all the polarization vectors that could exist at a plane interface between two *TI* media for the problem being considered here. It should be noted that $\sin\theta_\gamma \geq 0$ for all wave types, if the angle of the incident wave is such that $0 \leq \theta_{O(n)} \leq \pi/2$ where $\theta_{O(n)}$ being collinear with the vertical, x_3, axis corresponds to $\theta_{O(n)} = 0$.

The formulae for the polarization vectors $\mathbf{g}_{qS_V}$ appear to be the same as for $\mathbf{g}_{qP}$, however, the slowness vectors $\mathbf{p}$ are different for qP and qS_V wave type propagation in the same medium, and the polarization vectors are functions of these. This is discussed later.

Taking the paper of Farra and Pšenčík (2003) as an example, the components of the linearized qP polarization vector in a general anisotropic medium may be written as

$$g^{i}_{qP}\left(n_j\right) = n_i + \frac{B_{13}e_{1i}}{B_{33}-B_{11}} + \frac{B_{23}e_{2i}}{B_{33}-B_{22}} \tag{21}$$

In a TI medium, $B_{23}=0$ (Pšenčík and Gajewski, 1998), so that

$$g^{1}_{qP} = n_1 + \frac{B_{13}e_{11}}{B_{33}-B_{11}} = \sin\theta + \frac{B_{13}\cos\theta}{B_{33}-B_{11}} = \sin\theta + \Delta g^{1}_{qP} \tag{22}$$

$$g^{3}_{qP} = n_3 + \frac{B_{13}e_{13}}{B_{33}-B_{11}} = \cos\theta - \frac{B_{13}\sin\theta}{B_{33}-B_{11}} = \cos\theta - \Delta g^{3}_{qP} \tag{23}$$

In the initial derivation of the above formulae the quantities B_{33} and B_{11} were taken to be related to the isotropic qP and qS_V background velocities α and β, as $B_{33}=\alpha^2$ and $B_{11}=\beta^2$, respectively (Pšenčík and Gajewski, 1998). In the above, the vectors $\mathbf{n}$ and $\mathbf{e}_1$, and their degenerate TI forms were previously defined in equations (7) –(9).

As discussed earlier, it can be seen that $\mathbf{n}_{TI}=\left(\mathbf{e}_3\right)_{TI}$ and $\left(\mathbf{e}_1\right)_{TI}$ are an orthonormal vector couple in the $(1,3)$ plane. If the vector $\mathbf{e}_2$ is considered, the vector triplet $\left(\mathbf{e}_1,\mathbf{e}_2,\mathbf{e}_3\right)=\left(\mathbf{e}_1,\mathbf{e}_2,\mathbf{n}\right)$ is an orthonormal basis vector system in 3 dimensions. The vector $\mathbf{n}$ is often referred to as the phase or normal angle vector associated with the qP wave propagation in an anisotropic medium, (Figure 2).

As previously indicated, the quantities B_{mn} are defined by the relations

$$B_{mn} = \Gamma_{jk}e_{mj}e_{nk} \quad \text{with} \quad \Gamma_{jk} = a_{ijk\ell}n_i n_\ell \,. \tag{24}$$

The elements of the tensor $a_{ijk\ell}=c_{ijk\ell}/\rho$ are anisotropic coefficients defined in terms of the stiffnesses of a medium, $c_{ijk\ell}$, and density, ρ, which have equivalents in Voigt $\left(A_{ij}\right)$ notation having dimensions of velocity squared, as previously mentioned. For a TI medium the relevant $B_{mn}\left(B_{11},B_{33},B_{13}\right)$ may be written as

$$B_{11} = A_{55} - E_{13}\sin^2\theta\cos^2\theta \tag{25}$$

$$B_{33} = A_{11}\sin^2\theta + A_{33}\cos^2\theta + E_{13}\sin^2\theta\cos^2\theta \tag{26}$$

$$B_{13} = \frac{\sin\theta\cos\theta}{2}\left[\left(A_{11}-A_{33}\right) + E_{13}\left(1-2\sin^2\theta\right)\right] \tag{27}$$

Here B_{33} and B_{11} may be seen (see Pšenčík and Farra, 2005, as an example) to be the squares of the linearized qP and qS_V phase velocities, and the deviation from the elliptical in the linearized case is defined as

$$E_{13} = 2\left(A_{13} + 2A_{55}\right) - \left(A_{11} + A_{33}\right) \tag{28}$$

which is the complement of the anellipticity, A_D, in the general formulation, and is given by equation (19).

The qS_V equivalents of (22) and (23) are

$$g^1_{S_V} = e_{31} + \frac{B_{13}n_3}{B_{33} - B_{11}} = -\sin\theta + \frac{B_{13}\cos\theta}{B_{33} - B_{11}} = -\sin\theta + \Delta g^1_{S_V} \tag{29}$$

$$g^3_{S_V} = e_{11} + \frac{B_{13}n_1}{B_{33} - B_{11}} = \cos\theta + \frac{B_{13}\sin\theta}{B_{33} - B_{11}} = \cos\theta + \Delta g^3_{S_V} \tag{30}$$

(In the above the superscripts on the polarization vector components are defined to be consistent with those implied in Figure 2.) There remains a final matter to be considered before the above expressions may be incorporated into software for the computation of reflection and transmission coefficients. The exact and linearized cases discussed above have different forms of the eikonal equation for both the qP and qS_V waves. The eikonal equations are functions of the components of the slowness vector $\mathbf{p} = \left(p_1, p_3\right)$. As it is assumed that the horizontal component, p_1, of the slowness vector is known, it remains to determine the vertical component of the slowness vector p_3. In both cases, the solutions for p_3 are in terms of the anisotropic parameters of the medium, and p_1. The p_3 are solutions of quartic equations which are homogeneous in powers of p_3^2, given by

$$K_2 p_3^4 + K_1 p_3^2 + K_0 = 0, \quad p_3 = \sqrt{\frac{-K_1 + \sqrt{K_1^2 - 4K_2K_0}}{2}} \tag{31}$$

for the linearized case the where the coefficients $K_i \left(i = 0,1,2\right)$ are

$$\begin{aligned} K_2 &= A_{33} \\ K_1 &= \left(A_{11} + A_{33}\right)p_1^2 - E_{13}p_1^2 - 1 \qquad \left(qP\right) \\ K_0 &= A_{11}p_1^4 - p_1^2 \end{aligned} \tag{32}$$

and

$$\begin{aligned} K_2 &= A_{55} \\ K_1 &= 2A_{55}p_1^2 - E_{13}p_1^2 - 1 \qquad \left(qS_V\right) \\ K_0 &= A_{55}p_1^4 - p_1^2 \end{aligned} \tag{33}$$

In the exact case the quartic solution is

$$p_3 = \sqrt{\frac{-K_1 \mp \sqrt{K_1^2 - 4K_2K_0}}{2}} \quad ("-"qP, \quad "+"qS_V) \tag{34}$$

with

$$\begin{aligned} K_2 &= A_{33}A_{55} \\ K_1 &= 2A_{55}\left(A_{11}+A_{33}\right)p_1^2 - A_D p_1^2 - \left(A_{33}+A_{55}\right) \qquad (qP \text{ and } qS_V) \\ K_0 &= 1 + A_{11}A_{55}p_1^4 - \left(A_{11}+A_{55}\right)p_1^2 \end{aligned} \tag{35}$$

NUMERICAL RESULTS

A two layered model consisting of a highly anisotropic transversely isotropic halfspace overlying an isotropic halfspace was considered to produce numerical results. The anisotropic parameters defining these two media are given in Table 1. The upper medium has anisotropic parameters similar to the $(1-3)$ plane of olivine. It is assumed that in both media the invariant rotational axes are normal to the plane interface separating the media. The use of the isotropic lower halfspace was chosen so that parameters of the upper halfspace dominate the anisotropic effects seen in the graphical displays. The qP and qS_V ray (group) velocity and slowness surfaces for the upper medium are shown in Figure (3). These surfaces were computed using their exact parameterization. The qS_V critical angle in the upper medium is $\cong 23$ degrees.

Before proceeding, it may be instructive to compare the qP and qS_V polarization vector components for the exact and linearized cases. The real parts of these vector components are displayed in Figures (4) and (5); the imaginary parts being zero. The two components of the qP polarization vector are shown in Figure (4), plotted versus the $qP-$wave incident phase angle which varies from 0 to 90 degrees. Similar results for the qS_V polarization vector are shown in Figure (5) over the range of qS_V (sub-critical) phase angles from 0 to 23 degrees, The inputs to both the exact and linearized programs require that the horizontal component of the slowness vector be known. This is computed independently in each program. In all four panels in these figures, the black line refers to the exact solution, the grey line to the linearized solution, and the dotted line to the zero order solution, either $\sin\theta$ or $\cos\theta$. More detail may be found in the figure captions.

The amplitude and phase of the exact and linearized reflection coefficients, R_{P1P1} and R_{P1S1}, are displayed versus the qP - wave phase angle of incidence in Figures (6) and (7). As before, the black lines refer to the exact case, and the grey lines to the linearized formulation. Finally, the amplitude and phase of the R_{P1S1} reflection are plotted against the ray (group) angle of incidence in the upper medium in Figure (8). The effect of the triplication of the qS_V wave surface is quite evident in this plot. Further, the closeness of fit between the exact and linearized solutions is better than could be expected.

As a final example the R_{S1S1} reflection coefficient is considered. In a manner similar to the R_{P1P1} instance, the linearized and exact polarization vectors of the incident/ reflected qS_V wave are compared. The two components of these quantities are displayed in Figure (9) together with the zero order components $\left(\sin\theta_{qS_V}, \cos\theta_{qS_V}\right)$. Further discussion is given in the figure captions. The amplitude and phase of the exact and linearized reflection coefficient R_{S1S1}, are displayed versus the qS_V - wave phase angle of incidence in Figure (10). Again, for comparative purposes the exact and linearized, amplitudes and phases, are shown in Figure (11), plotted against the ray (group) incident/reflected angle. As might be expected from viewing Figure (3), the difference between the amplitudes and phases of the exact and linearized forms of R_{S1S1} are more pronounced in this example.

CONCLUSIONS

Given software that computes the exact reflection and transmission coefficients at an interface between two transversely isotropic media, additional software consisting of linearized phase velocities, eikonal equations and polarization vectors may be obtained and introduced into a similar program. This was undertaken as a preliminary exercise before addressing more complex situations such as reflection and transmission coefficients at the interface between two orthorhombic media to obtain some indication of any major problems that may arise. These linearized quantities are obtained using perturbation theory, and their range of validity should only include what has been termed "weak anisotropy". From the small numerical experiment presented here it could be concluded that this constraint could be exceeded. However, much more numerical testing should be done before any generalizations are made. The results obtained here provide enough incentive to extend this method to more complex anisotropic media types, specifically, orthorhombic symmetry. If the weak anisotropic limitation is imposed and adhered to, it may be supposed that the results obtained should be of reasonably accuracy.

Layer	A_{11}	A_{33}	A_{55}	A_{13}	A_D	$\tilde{A}_D = \sigma$	ε	ρ
1	14.8246	12.2080	1.3059	6.7032	-83.236	-0.3127	0.1071	2.0
2	25.0	25.0	7.4	10.2	0.0	0.0	0.0	2.2

Table 1. Anisotropic parameters, A_{ij}, used in computing the reflection coefficients. The units of all of these parameters is velocity squared $\left(km^2/s^2\right)$ except for A_D $\left(km^4/s^4\right)$ and the ellipticity, ε, and the measure of anellipticity, $\tilde{A}_D = \sigma$, which are dimensionless. The linearized anellipticity parameter, E_{13}, has the value for layer 1 of $-8.4026\,km^2/s^2$. In a dimensionless form, $\tilde{E}_{13} = E_{13}/2A_{33}$, the value is -0.3441. The densities, ρ, are in gm/cm^3.

REFERENCES

Backus, G.E., 1965, Possible forms of seismic anisotropy of the uppermost mantle under oceans, Journal of Geophysical Research, 70, 3429-3439.

Červený, V., 2001, Seismic Ray Theory: Cambridge University Press, Cambridge.

Daley, P.F. and Hron, F., 1977, Reflection and transmission coefficients for transversely isotropic media, Bulletin of the Seismological Society of America, 64, 954-962.

Farra, V., and Pšenčík, I., 2003, Properties of the zero-, first- and higher-order approximations of attributes of elastic waves in weakly anisotropic media: Journal of the Acoustical Society of America, 114, 1366-1378.

Farra, V. and Pšenčík, I., 2008, First-order ray computations of coupled S waves in inhomogeneous weakly anisotropic media, Geophysical Journal International, 173, 979-989.

Gassmann, F., 1964, Introduction to seismic travel time methods in anisotropic media, Pure and Applied Geophysics, 58, 63-113.

Graebner, M., 1992, Plane-wave reflection and transmission coefficients for a transversely isotropic solid, Geophysics, 57, 1512-1519.

Jech, J. and Pšenčík, I., 1989, First – order perturbation method for anisotropic media, Geophysical Journal International, 99, 369-376.

Mensch, T. and Rasolofosaon, P., 1997, Elastic wave velocities in anisotropic media of arbitrary anisotropy – generalization of Thomsen's parameters ε, δ and γ, Geophysical Journal International, 128, 43-64.

Pšenčík, I. and Farra, V., 2005, First – order ray tracing for qP waves in inhomogeneous weakly anisotropic media, Geophysics, 70, D65-D75.

Pšenčík, I. and Gajewski, D., 1998. Polarization, phase velocity and NMO velocity of qP waves in arbitrary weakly anisotropic media, Geophysics, 63, 1754-1766.

Sayers, C.M., 1994, P – wave propagation in weakly anisotropic media, Geophysical Journal International, 116, 799-805.

Schoenberg, M., and Helbig, K., 1997, Orthorhombic media: Modeling elastic wave behavior in a vertically fractured earth: Geophysics, 62, 1954-1974.

Thomsen, L., 1986, Weak elastic anisotropy, Geophysics, 51, 1954-1966.

ACKNOWLEDGEMENTS

The support of the sponsors of CREWES is duly noted. The first author also receives assistance from NSERC through operating and strategic grants held by Professors E.S. Krebes, L.R. Lines and G. F. Margrave.

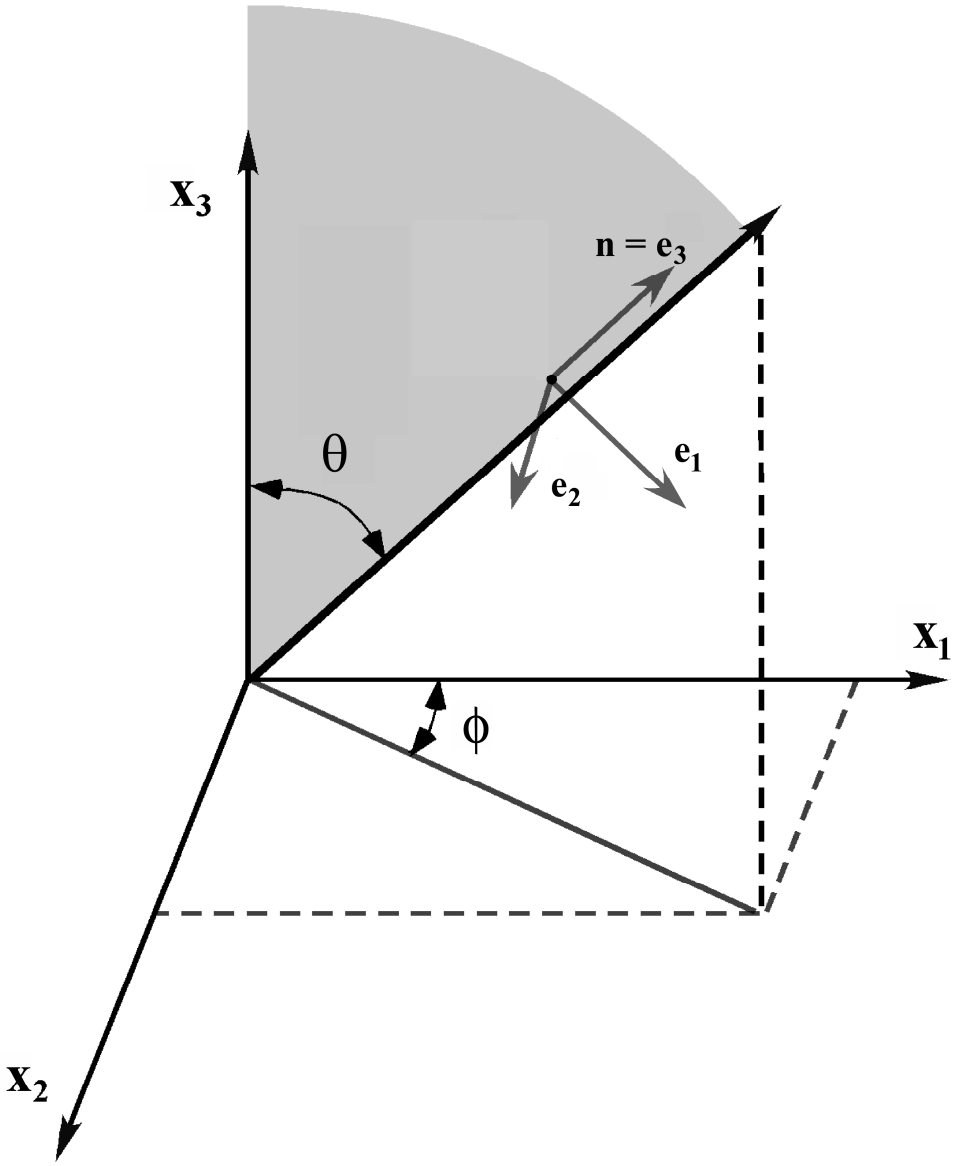

FIG. 1. Orthonormal triad of vectors $(\mathbf{e}_1, \mathbf{e}_2, \mathbf{e}_3 = \mathbf{n})$. The choice of the orientation of the orthonormal vector pair $(\mathbf{e}_1, \mathbf{e}_2)$ which spans a plane normal to $\mathbf{e}_3 = \mathbf{n}$ is arbitrary. However, for the problem being considered here, $\mathbf{e}_1$ has been chosen to be oriented in such a manner that it and $\mathbf{e}_3 = \mathbf{n}$ form the plane of ray propagation for a transversely isotropic medium. This degenerate arrangement allows the angle ϕ to also be arbitrary. Consequently, it is chosen equal to zero so that $\mathbf{e}_2$ is normal to the $(\mathbf{e}_1, \mathbf{e}_3)$ plane and can be taken to describe the direction of particle displacement of the qS_H wave.

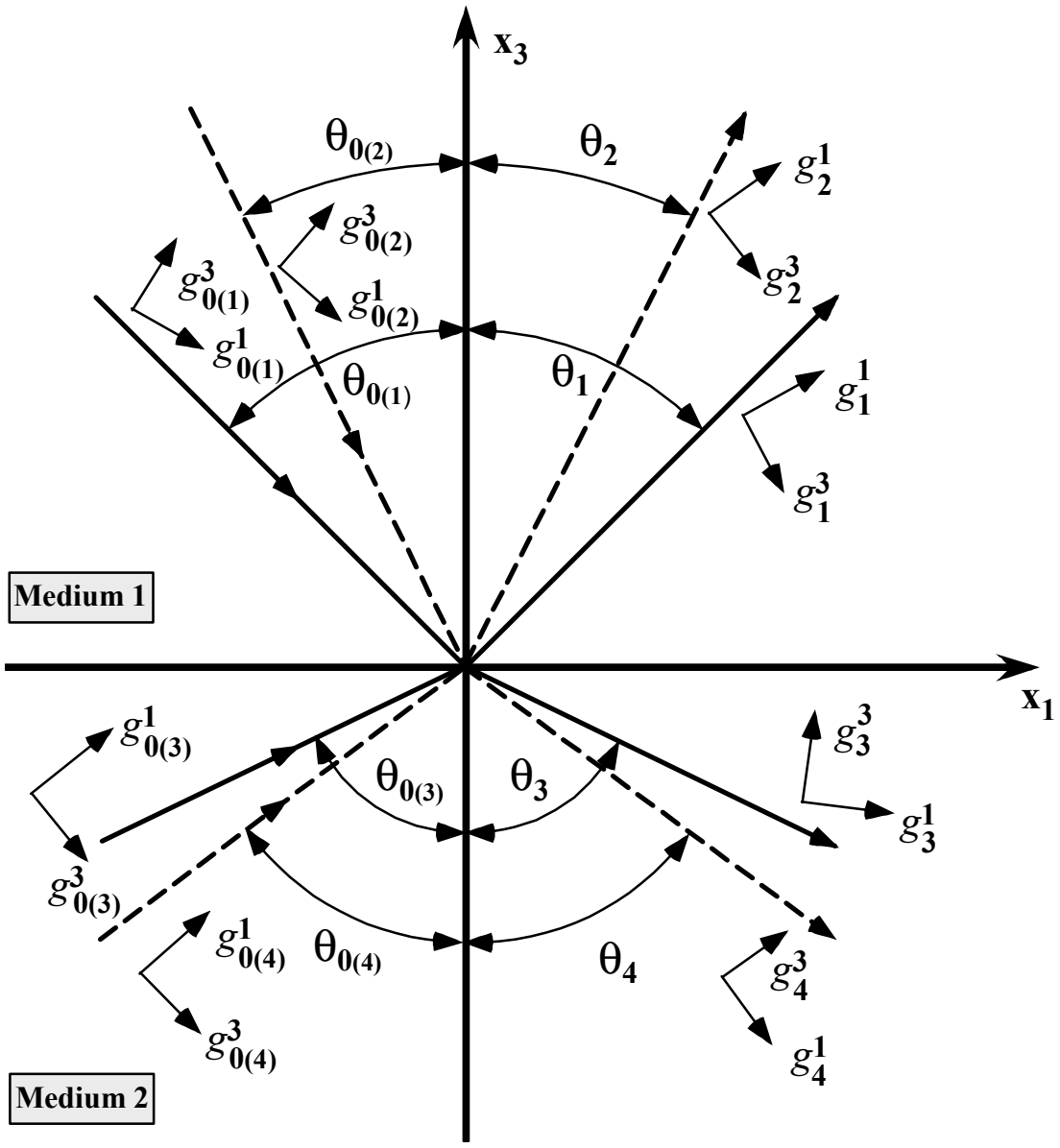

FIG. 2. The geometry of the 4 types of incident wavefronts at an interface between two transversely isotropic media together with the 4 possible reflected and transmitted wave types. The subscripts ς on θ_ς and g^i_ς indicates an incident wavefront type if it is the form $O(n)$, where $n=1$ refers to a qP wave in the upper (1) medium, $n=2$ to a qS_V wave in the upper (1) medium, $n=3$ to a qP wave in the lower (2) medium and $n=4$ to a qS_V wave in the lower (2) medium. The orientations of the vector components g^1_ς and g^3_ς are the same as those used in both program types – exact and linearized. It should be noted that the positive direction of the vertical axis has been chosen upwards.

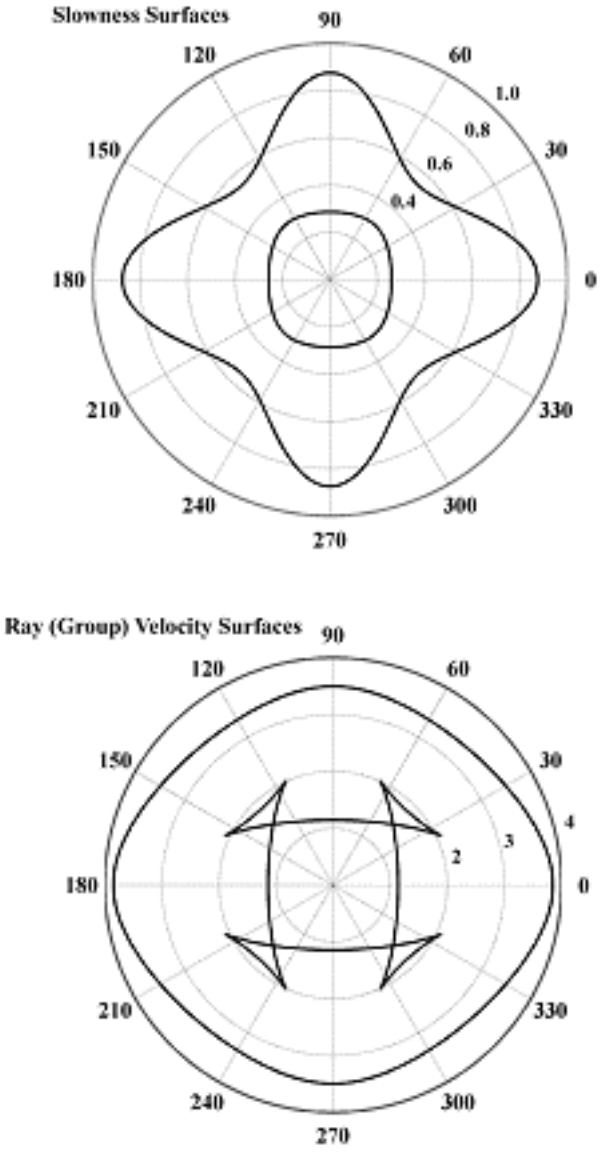

FIG. 3. Plots in the polar domain of the slowness and ray surfaces of the qP and qS_V wave types of the upper medium. The dimensions of the markers on the slowness surfaces plots are s/km while those for the ray surfaces are km/s. It is clear from viewing these surfaces that the medium chosen is not what could be classified as weakly anisotropic. This model is specified by using a slight modification of the anisotropic parameters defining the $(1,3)$ plane in olivine.

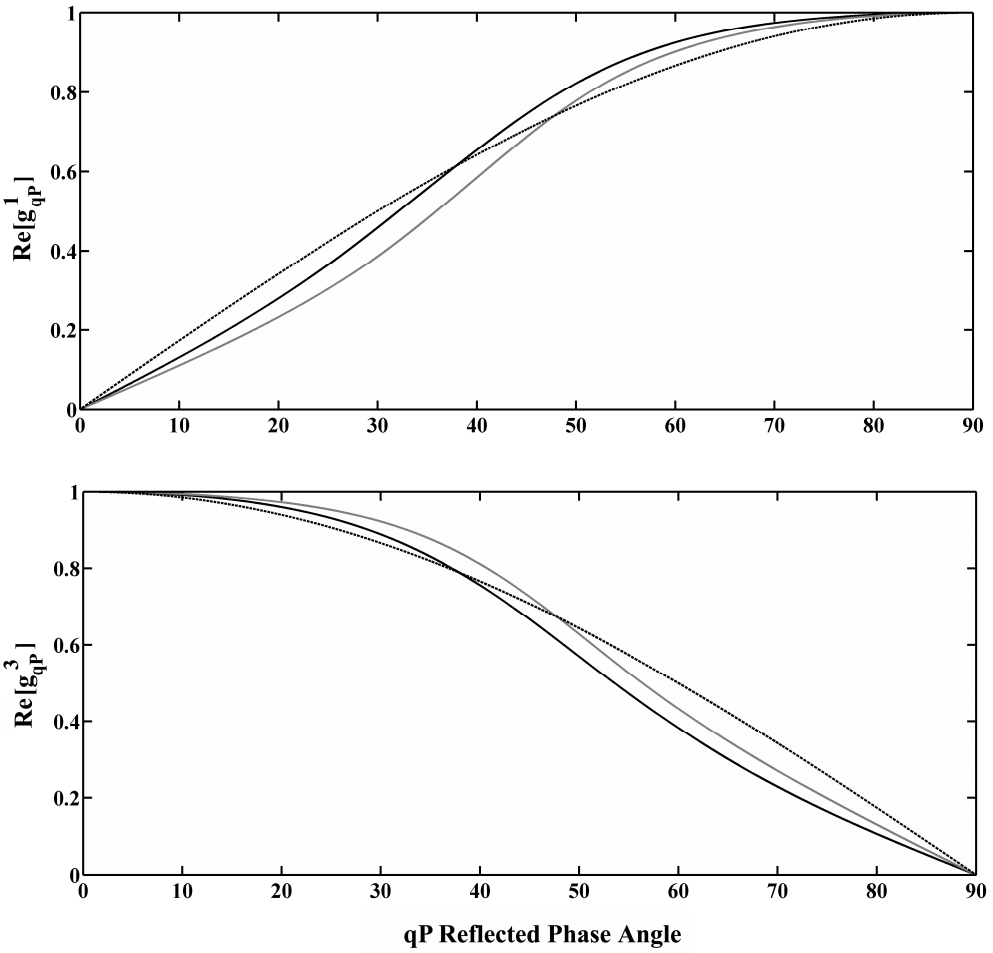

FIG. 4. A comparison of the real parts of the vector components g^1_{qP} (top) and g^3_{qP} (bottom) for the reflected qP wave type plotted versus the reflected qP phase angle for the R_{P1P1} reflection coefficient. The imaginary parts of these two quantities are zero. The exact cases are plotted in black, the linearized cases in grey, and the reference curve, either $\sin\theta_{qP}$ or $\cos\theta_{qP}$, is shown by the dotted line.

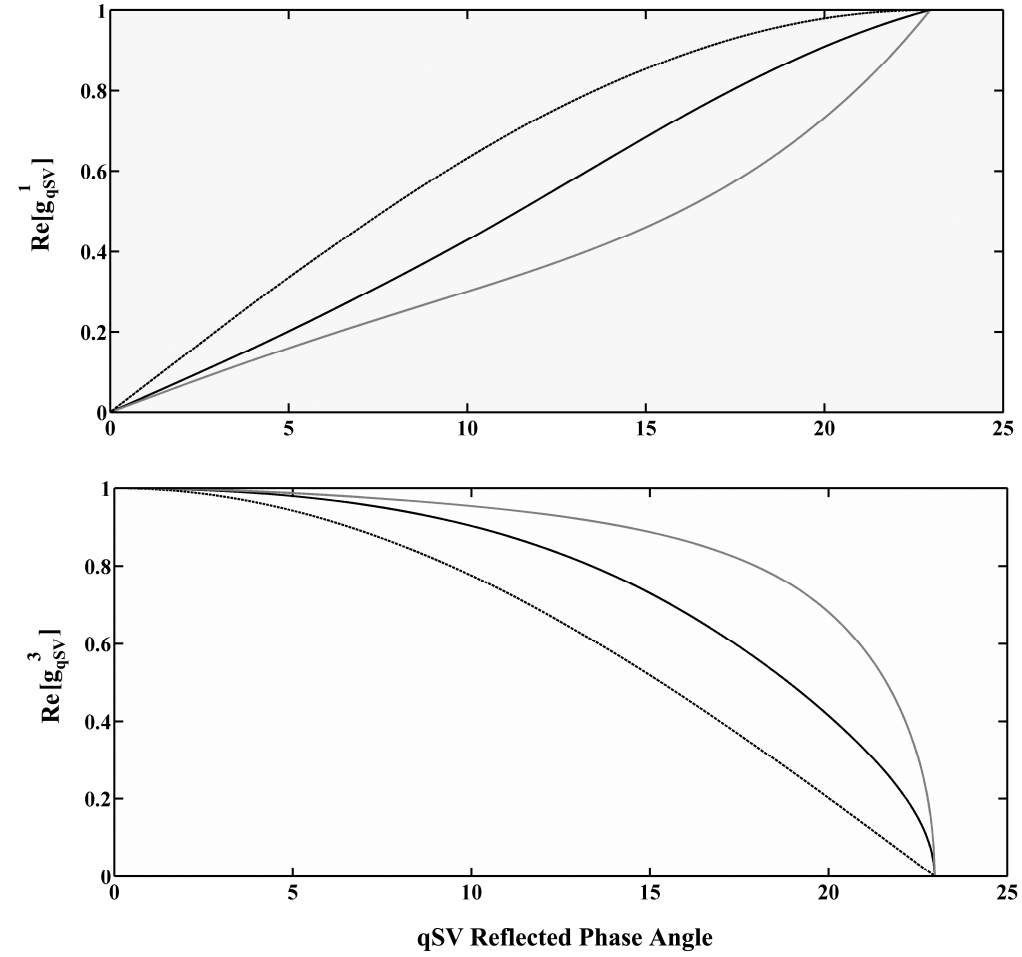

FIG. 5. A comparison of the real parts of the vector components g^1_{qP} (top) and g^3_{qP} (bottom) for the reflected qS_V wave type, due to qP wave incidence in the upper medium, plotted versus the reflected qS_V phase angle. As mentioned in the text, the imaginary parts of these two quantities are zero. The exact cases are plotted in black, linearized in grey, and the reference curve, either $\sin\theta_{qS_V}$ or $\cos\theta_{qS_V}$, is shown by the dotted line. As grazing incidence of the qP wave corresponds to $\theta_{qS_V} \cong 23$ degrees, the upper bound for the qS_V phase angle axes in this case is 23 degrees. The fit of the exact with the linearized case is not as good here as in the qP case in the previous figure, and the deviation of both from the zeroth order curves is also greater than in figure 3. There is no immediate explanation for this.

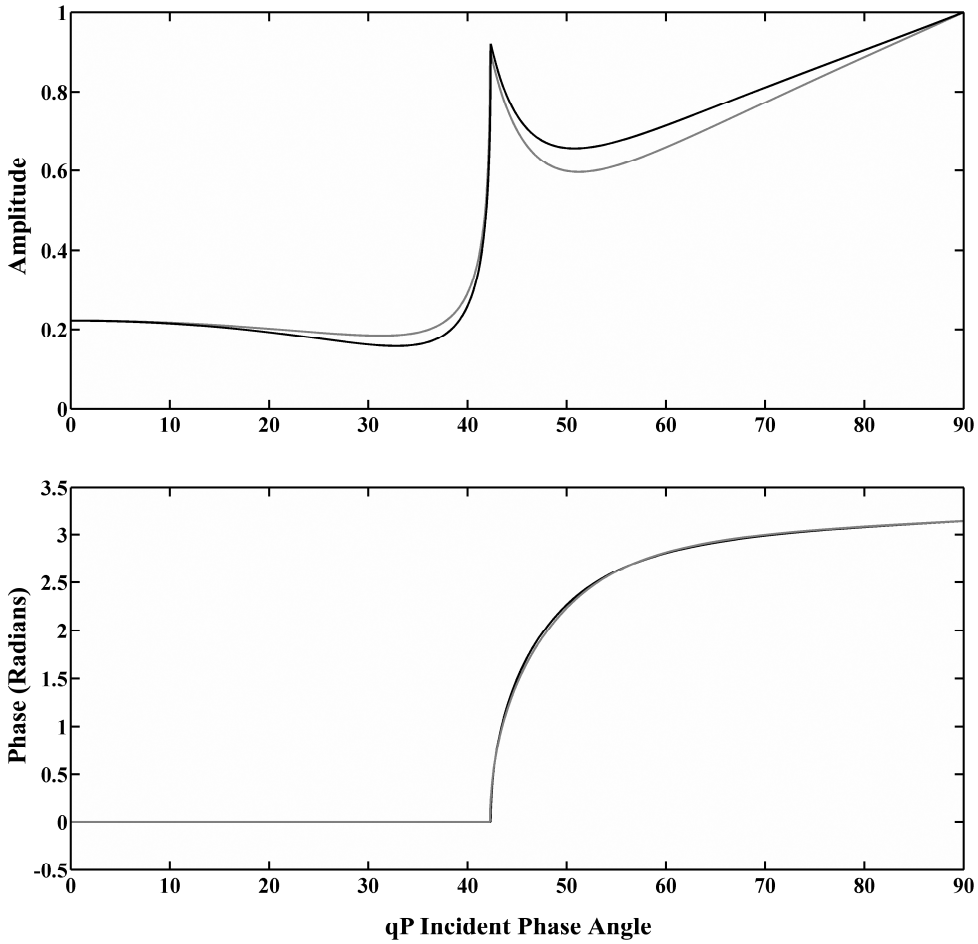

FIG. 6. The reflection coefficient R_{P1P1} due to a qP plane wave incident from the upper medium. The amplitude and phase of the reflection coefficient is plotted against the incident qP phase angle. The media parameters are those given in Table 1. As in previous figures, the black line corresponds to the exact case, grey to the linearized case.

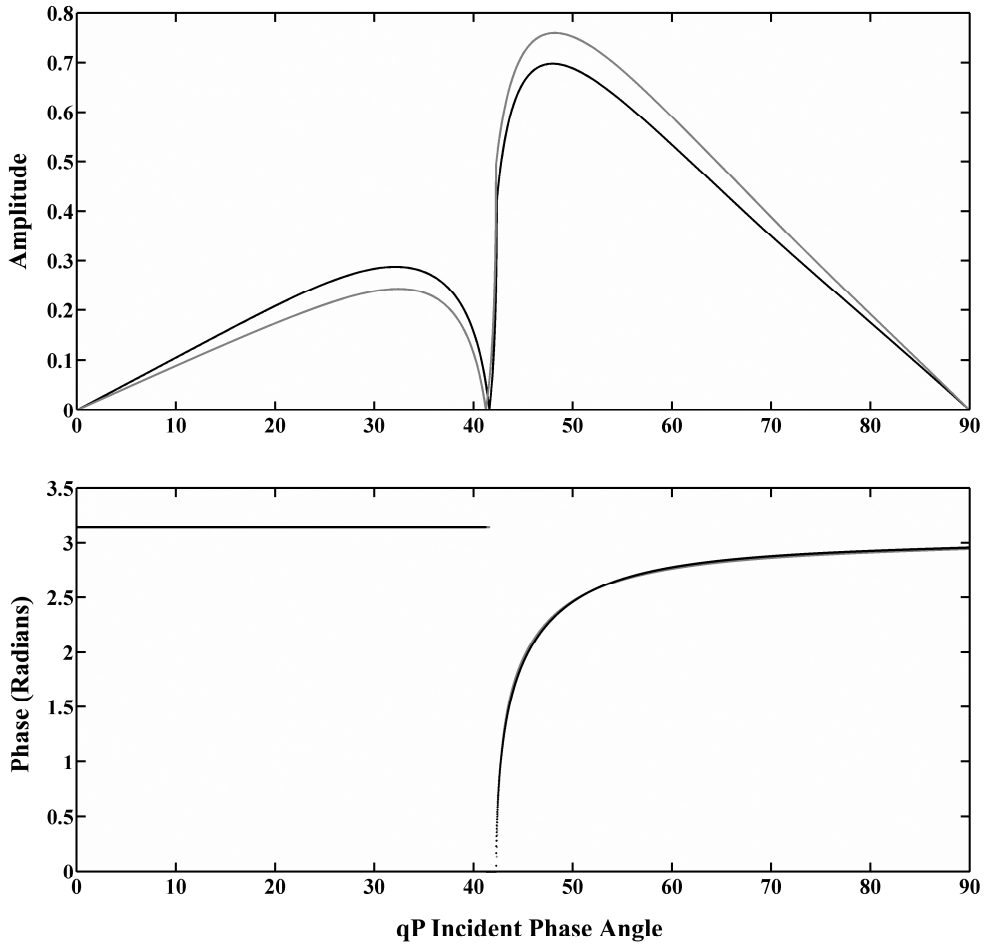

FIG. 7. The reflection coefficient R_{P1S1} due to a qP plane wave incident from the upper medium. The amplitude and phase of the reflection coefficient is plotted against the incident qP phase angle. The media parameters are those given in Table 1. The black line corresponds to the exact case, grey to the linearized case as in previous figures.

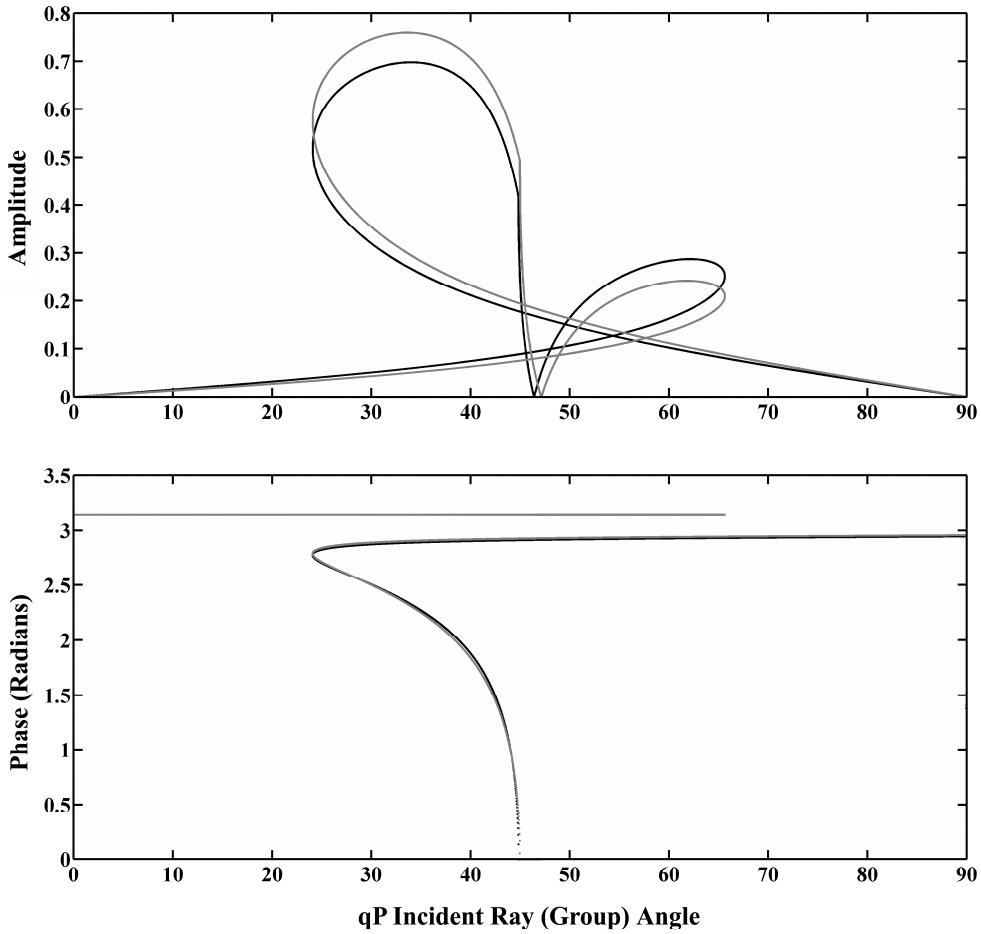

FIG. 8. The reflection coefficient R_{P1S1} due to a qP plane wave incident from the upper medium, where the amplitude and phase is plotted versus the incident qP group angle. As is clear from the plotted curves, this was done as another check of how well the exact and linearized reflected qS_V amplitudes and phases of the exact and linearized cases matched. Again, the exact curves are black and the linearized curves are grey.

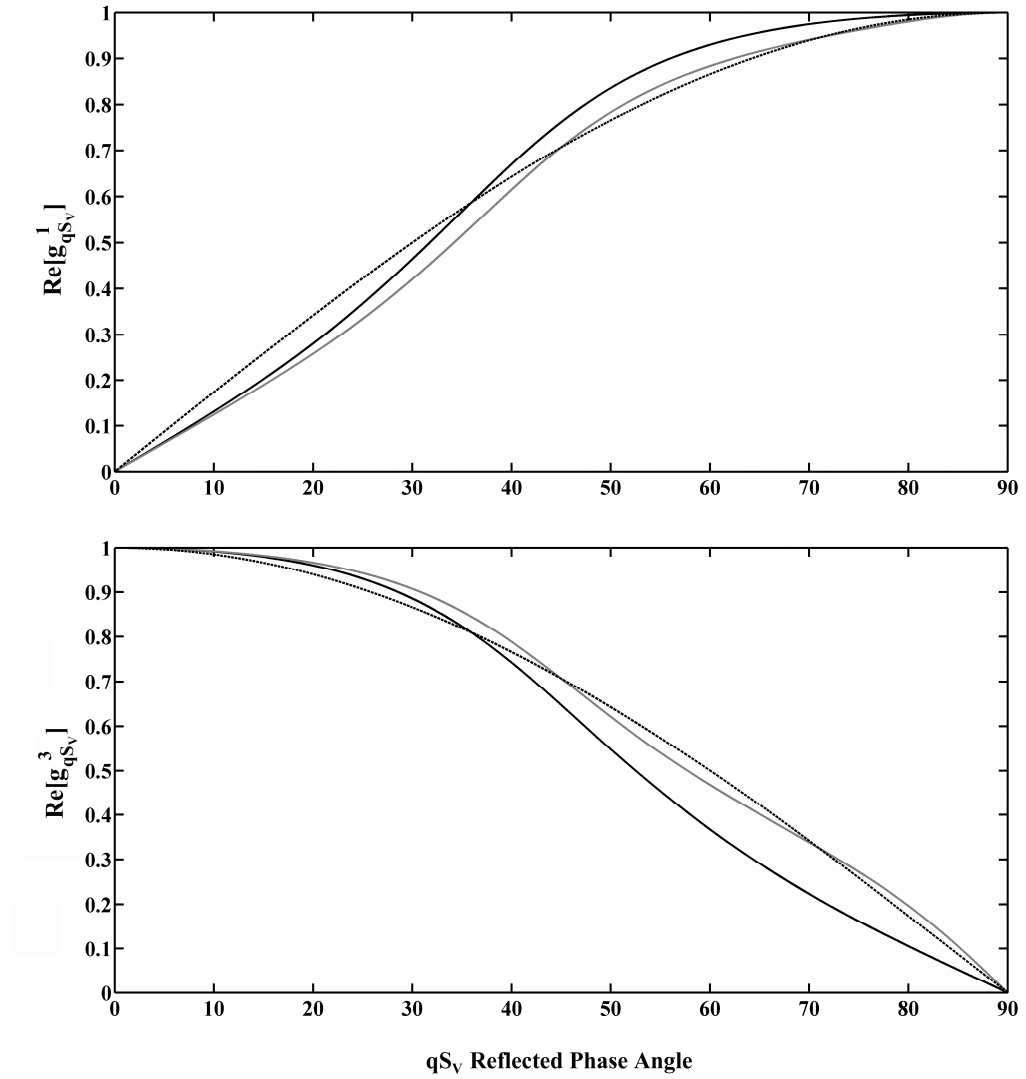

FIG. 9. A comparison of the real parts of the vector components $g^1_{qS_V}$ (top) and $g^3_{qS_V}$ (bottom) for the reflected qS_V wave type plotted versus the reflected qS_V phase angle for the R_{S1S1} reflection coefficient. The imaginary parts of these two quantities are zero. The exact cases are plotted in black, the linearized cases in grey, and the reference curve, either $\sin\theta_{qS_V}$ or $\cos\theta_{qS_V}$, is shown by the dotted line.

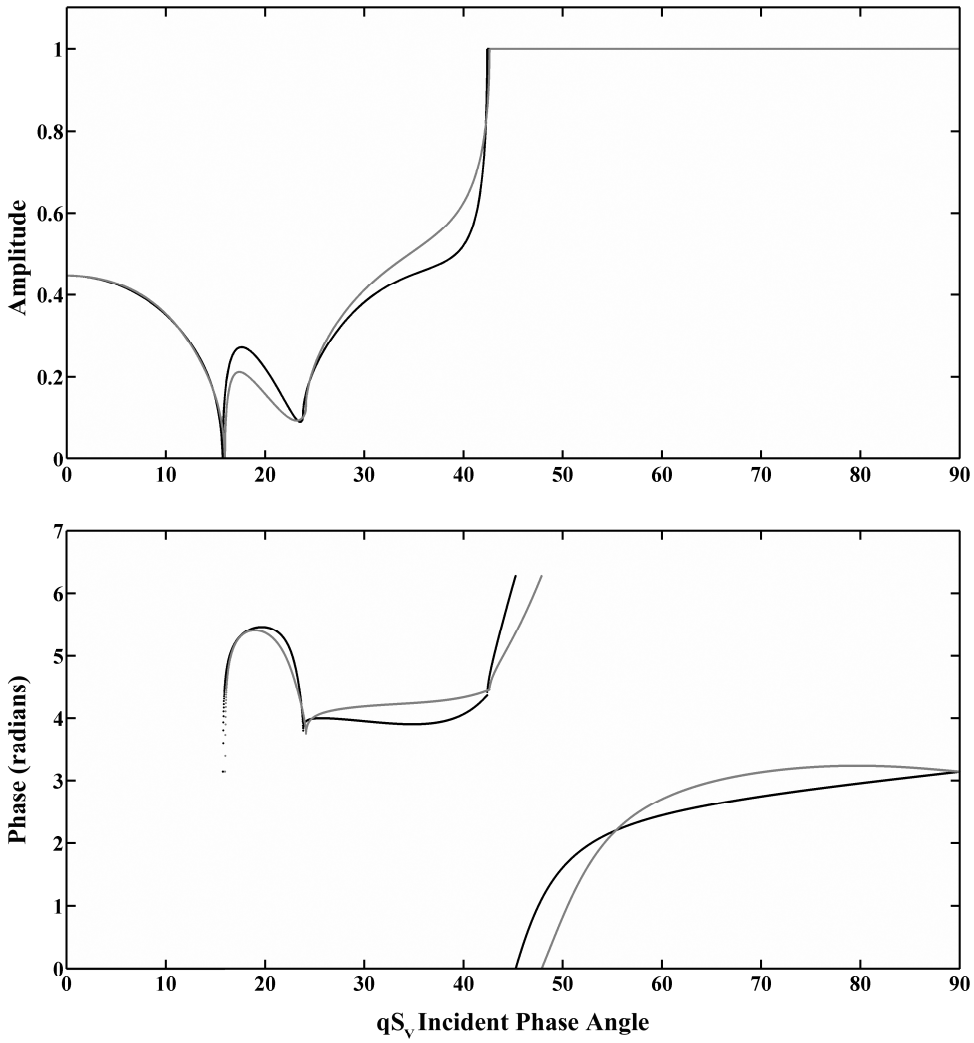

FIG. 10. The reflection coefficient R_{S1S1} due to a qS_V plane wave incident from the upper medium. The amplitude and phase of the reflection coefficient is plotted against the incident qS_V phase angle. The media parameters are those given in Table 1. The black line again corresponds to the exact case and grey to the linearized case.

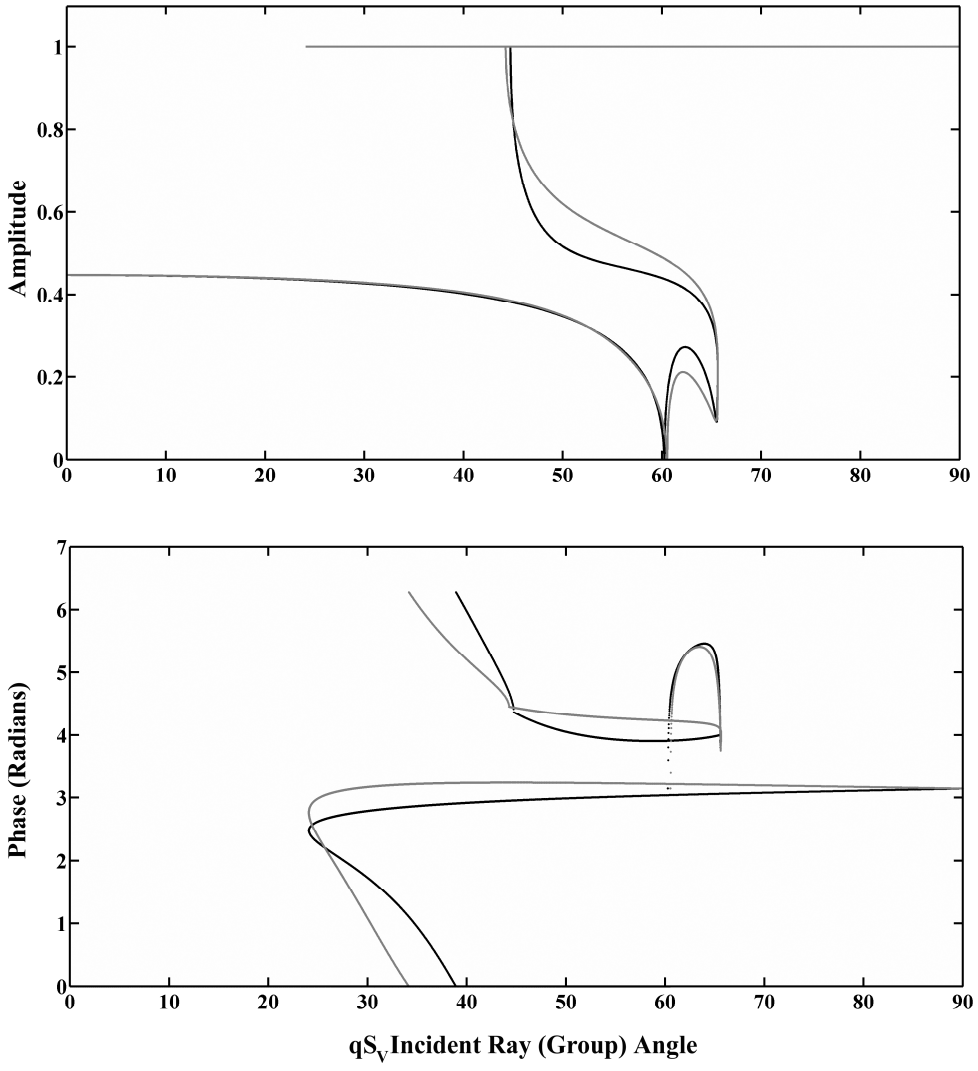

FIG. 11. The reflection coefficient R_{S1S1} due to a qS_V plane wave incident from the upper medium where the amplitude and phase is plotted versus the incident qS_V group angle. As is clear from the plotted curves, this was done as an extra check of how well the exact and linearized reflected qS_V amplitudes and phases of the exact and linearized cases matched. The exact curves are black and the linearized curves are grey.